

COMMUNICATION

Homology in Structural Organization Between *E. coli* ClpAP Protease and the Eukaryotic 26 S Proteasome

Martin Kessel^{*1,4}, Michael R. Maurizi^{2*}, Bernard Kim¹, Eva Kocsis¹
Benes L. Trus^{1,3}, Satyendra K. Singh² and Alasdair C. Steven¹

¹Laboratory of Structural Biology, National Institute of Arthritis and Musculoskeletal and Skin Diseases

²Laboratory of Cell Biology National Cancer Institute, and

³Computational and Biosciences Engineering Laboratory, Division of Computer Research and Technology, National Institutes of Health, Bethesda MD 20892, USA

⁴Department of Membrane and Ultrastructure Research Hebrew University-Hadassah Medical School, Jerusalem Israel

Energy-dependent protein degradation is carried out by large multimeric protein complexes such as the proteasomes of eukaryotic and archaeal cells and the ATP-dependent proteases of eubacterial cells. Clp protease, a major multicomponent protease of *Escherichia coli*, consists of a proteolytic component, ClpP, in association with an ATP-hydrolyzing, chaperonin-like component, ClpA. To provide a structural basis for understanding the regulation and mechanism of action of Clp protease, we have used negative staining electron microscopy and image analysis to examine ClpA and ClpP separately, as well as active ClpAP complexes. Digitized images of ClpP and ClpA were analyzed using a novel algorithm designed to detect rotational symmetries. ClpP is composed of two rings of seven subunits superimposed in bipolar fashion along the axis of rotational symmetry. This structure is similar to that formed by the beta subunits of the eukaryotic and archaeal proteasomes. In the presence of MgATP, ClpA forms an oligomer with 6-fold symmetry when viewed *en face*. Side views of ClpA indicate that the subunits are bilobed with the respective domains forming two stacked rings. ClpAP complexes contain a tetradecamer of ClpP flanked at one or both ends with a hexamer of ClpA, resulting in a symmetry mismatch between the axially aligned molecules. Our findings demonstrate that, despite the lack of sequence similarity between ClpAP and proteasomes, these multimeric proteases nevertheless have a profound similarity in their underlying architecture that may reflect a common mechanism of action.

© 1995 Academic Press Limited

Keywords: Clp protease; ATP-dependent protease; proteasome; rotational symmetry; image analysis

*Corresponding authors

Energy-dependent proteases play essential roles in degrading regulatory proteins during normal growth and development and under conditions of stress, and serve an essential housekeeping function by disposing of damaged or denatured proteins (Gottesman & Maurizi, 1992; Hershko & Ciechanover, 1992). In eukaryotic cells, proteins are targeted for degradation by covalent attachment of ubiquitin and the ubiquitinated proteins are digested by a high molecular weight, multimeric protease called the 26 S proteasome. The 26 S proteasome is composed of a non-ATP-dependent proteolytic component called the 20 S proteasome and a 19 S complex of regulatory proteins including one or more ATPases. A protein evolutionarily related and structurally similar to the 20 S proteasome is found in the archaean, *Thermoplasma*. Eubacteria, such as *Escherichia coli*, contain at least two soluble ATP-dependent proteases: Lon protease,

a high molecular weight oligomer of identical subunits, and Clp protease, a modular enzyme composed of a peptidase, ClpP, associated with one of several possible ATP-binding components, e.g. ClpA, that activate and confer specificity to the proteolytic activity.

The complexity of ATP-dependent proteases reflects the regulatory and mechanistic imperatives of carrying out efficient and rapid degradation of specific protein targets while avoiding damage to functional cellular proteins. The energy expended by ATP-dependent proteases is used for unfolding appropriate targets and translocating them into the proteolytic active sites (Gottesman & Maurizi, 1992). These dual functions are clearly evident for the ATP-dependent ClpAP protease from *E. coli*, which has recently been shown to have a molecular chaperone function in addition to its activity in promoting ATP-dependent protein turnover

(Wickner *et al.*, 1994). This enzyme serves as an excellent model for studying the mechanistic and physiological aspects of the link between protein remodeling and protein degrading activities necessary to protect cells from the deleterious effects of proteins with abnormal structures.

The ClpAP protease is formed from the association of ClpP, the protease, with ClpA, the ATPase (Gottesman & Maurizi, 1992; Maurizi, 1992). ClpA and ClpP can be purified separately and combined to reconstitute the active proteolytic complex (Maurizi, 1992). ClpP (subunit M_r 21,500) is an oligomeric protein that appears in electron micrographs as a donut-shaped particle with a diameter of ~ 11 nm (Maurizi *et al.*, 1990a). Micrographs showing fields of well stained molecules (e.g.

Figure 1a) were digitized and analyzed for rotational symmetry using a novel algorithm designed to detect subtly expressed rotational symmetries that are difficult to see in the presence of noise typically present in electron micrographs (Kocsis *et al.*, 1995). In each of four independent data sets (Table 1), an unequivocal 7-fold symmetry was detected; this signal was strongest around the outer rim of the particles. No other statistically significant symmetry was detected, and in particular there was no indication of 6-fold symmetry. Averaged images obtained after rotational and translational alignment, but not rotationally averaged, show a regular 7-fold-symmetric particle, with heavy stain accumulation in its center (e.g. Figure 1d). Essentially the same image was obtained by separately averaging

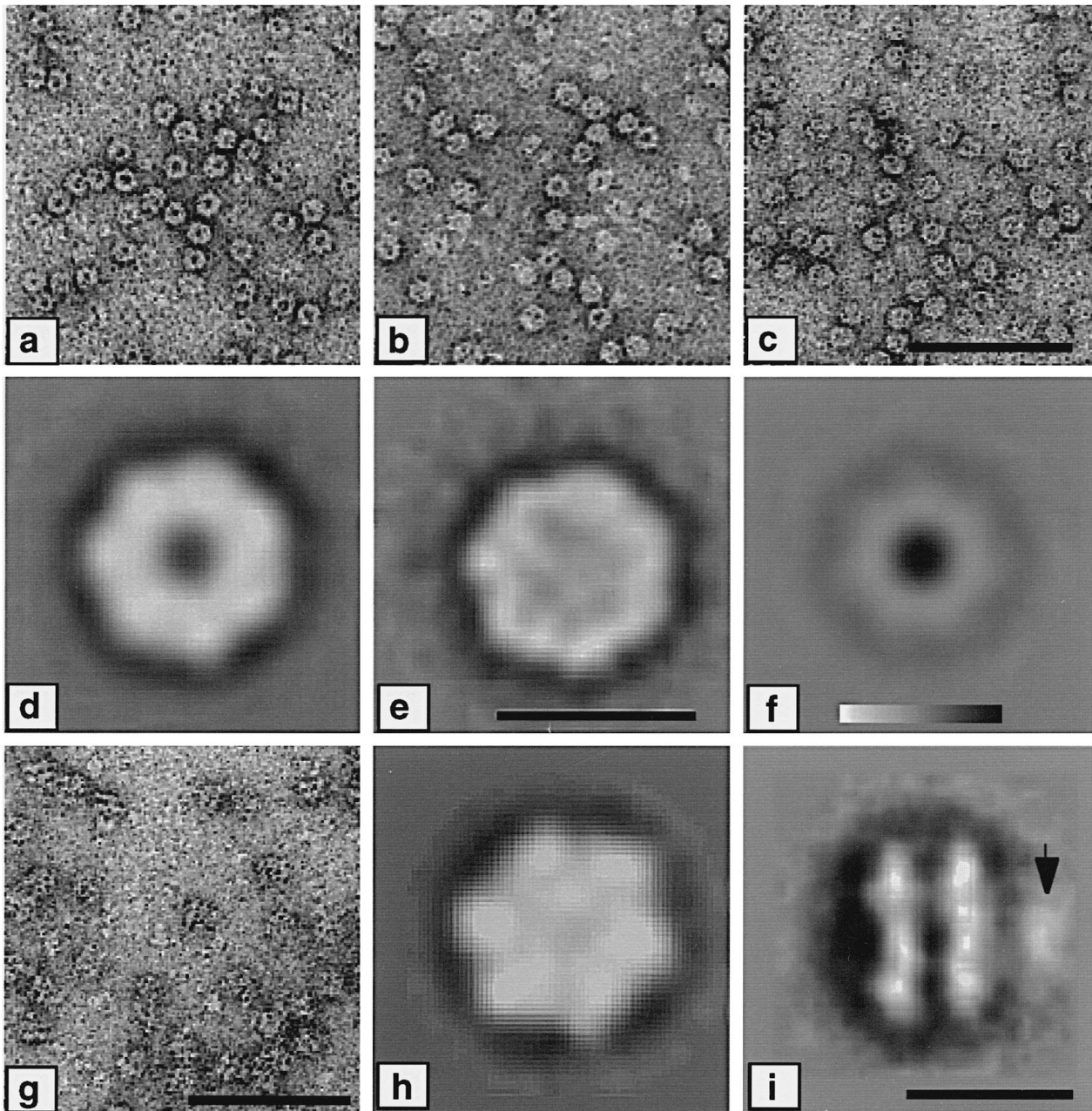


Figure 1 (legend opposite)

three other data sets in the same way (not shown). Thus the ClpP oligomer contains a multiple of seven subunits. In view of its M_r of 270,000 to 300,000 as determined by analytical ultracentrifugation (Maurizi & Ginsburg, 1995), ClpP must consist of two rings of seven subunits stacked along the axis of symmetry.

We also examined ClpP(SA), a mutant which retains the amino-terminal 14 amino acid propeptide (Maurizi *et al.*, 1990b) and forms an oligomer with a slightly higher M_r than that of ClpP (Maurizi & Ginsburg, 1995). An averaged view of ClpP(SA) is shown in Figure 1e. Its edges delineate a regular seven-sided particle, essentially indistinguishable in size and shape from ClpP: however, unlike ClpP, there is a conspicuous absence of stain accumulation in its center. This difference was also evident in micrographs of an approximately equimolar mixture of the two proteins (Figure 1b), and was confirmed quantitatively by a supervised classification analysis. In this experiment, the subpopulations of stain-accumulating molecules (~70%) and non-stain-accumulating molecules (~30%) from the same micrograph were separately averaged and then used as references to classify data sets of ClpP alone, and of ClpP(SA) alone. The latter data (165 images) correlated more strongly with the non-stain-accumulating reference with 100% fidelity, indicating that negative stain rarely if ever penetrates ClpP(SA) in amounts comparable to ClpP. The ClpP data ($N = 165$) correlated more strongly with this

reference in only 10% of cases, confirming that negative stain usually strongly penetrates the center of ClpP. We conclude, therefore, that the observed difference was not a fortuitous result of staining conditions: rather, it reflects stain occlusion by the presence of additional mass (~24,000 Da) from the propeptides in the center of ClpP(SA).

A difference map calculated from averaged images of ClpP and ClpP(SA) (Figure 1f) shows the strong central stain accumulation in ClpP that is absent from ClpP(SA). There also appears to be a relatively faint ring of positive density around this central region. This feature may be indicative of conformational differences between the respective molecules, but its visibility is somewhat dependent on the relative scaling of the two images compared and it may well simply arise from slight differences in staining.

In the presence of ATP or a non-hydrolyzable analog of ATP, ClpA (subunit M_r 84,000) assembles into an oligomer of 450,000 to 500,000 Da (Maurizi, 1992; Singh & Maurizi, 1994). Micrographs of ClpA in the presence of ATP γ S and Mg (Figure 1g) show particles that are considerably more variable in appearance than ClpP, presumably representing a wider range of views and a greater lability. However, they include two distinctive projections: regularly shaped particles, ~13 nm in diameter, that are relatively infrequent and which we take to be *en face* views; and particles whose most prominent features are two parallel striations ~13 nm long and ~11 nm in combined width, with an additional "fuzzy" mass

Figure 1. Electron micrographs of ClpP, ClpP(SA), and ClpA. The proteins were purified by published methods and identified by enzymatic assay and Western blotting with anti-ClpP and anti-ClpA antibodies (Maurizi *et al.*, 1994). Specimens for electron microscopy were prepared by placing 5 μ l aliquots (100 μ g/ml protein in 50 mM Tris-HCl (pH 7.5), 1 mM EDTA, 1 mM DTT, 0.3 M KCl, and 10% (v/v) glycerol) on freshly glow-discharged carbon-coated collodion-covered grids for 30 seconds after which excess buffer was blotted off with filter paper. 5 to 10 drops of an aqueous solution of 1% (w/v) uranyl acetate were applied sequentially to the grids, excess stain was blotted off, and the grids allowed to dry. Specimens were viewed in a Philips EM400T transmission electron microscope operating at 80 kV. Micrographs were recorded on Kodak SO163 emulsion at a nominal magnification of 60,000 \times . a, A typical field of wild-type ClpP molecules. Bar represents 50 nm (also applies to b, c, g). b, A mixed population of wild-type ClpP and ClpP(SA), a mutant that retains the amino-terminal 14-residue propeptide normally removed from mature ClpP. c, A field of ClpP(SA) molecules. d, Averaged image of ClpP viewed in *en face*. e, Averaged image of ClpP(SA), *en face* projection. In calculating image d, a data set of 216 images was screened to remove (anomalous) outliers by the OMO algorithm (Unser *et al.*, 1986), and the remaining 177 images were averaged. The average in e was calculated in the same way as in d. Bar represents 10 nm (also applies to d, f). f, Difference map calculated between the images shown in d and e, respectively, after rotational alignment and 7-fold rotational symmetrization and scaling as described by Carrascosa & Steven (1978). The background grey-level represents zero difference; darker tones denote enhanced stain penetration in ClpP compared to ClpP(SA), and *vice versa* for lighter tones; cf. inset linear greyscale. For image processing, micrographs were digitized with a Perkin-Elmer 1010G flatbed microdensitometer at a scanning rate corresponding to 0.5 nm per pixel. General image processing and display operations were carried out using the PIC system of software (Trus *et al.*, 1992), implemented on an Alpha workstation (Digital Equipment Corp., Maynard, MA). Particles were interactively extracted from 1024 \times 1024 pixel fields displayed on the workstation monitor. The molecules were translationally aligned and subjected to a rotational power spectrum analysis, as described by Kocsis *et al.* (1995). The resolutions of the averaged images were determined according to the spectral signal-to-noise-ratio (SSNR) criterion (Unser *et al.*, 1987), see Table 1. g, A typical field of ClpA molecules. Oligomeric ClpA was formed by adding 2 mM ATP γ S and 20 mM MgCl₂ to a solution of 100 μ g/ml ClpA in the buffer described above. The molecules present two predominant projections of similar cross-sectional area: roundish particles (interpreted as *en face* views) and particles with two parallel electron-transparent striations (interpreted as side views). h, Averaged *en face* projection of ClpA obtained as described above (data set ClpA-2 in Table 1). The 6-fold symmetry is evident around the edges of the particle, and this aspect of its structure was reproduced in a second independent average (not shown). Inside the molecular periphery, the signal was not strong enough to register statistically significant 6-fold symmetry, and few details were visualized in this part of the image. i, Averaged side view of ClpA (data set ClpA-1 in Table 1). It shows a slightly unequal distribution of mass between the two striations. The polarity of the molecule is accentuated by the presence of a smaller, less contrasted, mass adjacent to the right-hand striation (arrow). Bar represents 10 nm (also applies to h).

Table 1. Image analysis of ClpP, ClpA, and ClpAP complexes

Sample	Total particles analyzed	Spectral ratio product ^a	Particles selected by OMO ^b	Resolution of averaged image (nm) ^c
A. Analyses of ClpP showing 7-fold symmetry				
ClpP-1 ^d	98	2.6×10^{14}	73	2.8
ClpP-2	147	9.6×10^{21}	116	2.2
ClpP-3	149	3.1×10^{27}	116	2.2
ClpP-4	165	4.4×10^{12}	124	2.7
ClpP(SA)-1 ^d	90	1.9×10^7	70	3.3
ClpP(SA)-2	84	2.5×10^6	64	2.2
B. Analyses of ClpA showing 6-fold symmetry				
ClpA-1 ^d	82	8.7×10^{20}	65	4.3
ClpA-2	89	1.0×10^{29}	61	2.7
ClpA-1 ^d (side view)	63	NA ^g	38	3.5
ClpA-2 (side view)	54	NA	45	2.8
C. Analyses of ClpAP complexes				
2:1 ClpAP-1 ^{d,e}	90	..	68	3.0
-2	85	..	61	3.6
2:1 ClpAP(SA)	80	..	57	3.5
1:1 ClpAP ^f	94	..	65	3.1

^a The data sets were analyzed for rotational symmetry by two algorithms (Kocsis *et al.*, 1995). The first calculates a "spectral ratio product" which is the product, over all the particles in the data set, of the ratio of the amplitude of a given component of a particle's rotational power spectrum and the average of this component for background areas of the same micrograph. If a symmetry is present in a given particle, this ratio should be >1. This ratio is calculated for each rotational frequency, i.e. each potential order of rotational symmetry, in each radial zone, separately. If a symmetry is consistently present, the corresponding product diverges to large values as the number of particles increases; otherwise, it converges towards zero. The Table lists the values of the products for all symmetries which were detected as statistically significant (7-fold for ClpP and 6-fold for ClpA). The radial zones in which these symmetries were detected most strongly were 5.0 to 5.5 nm for ClpP and 6.0 to 6.5 nm for ClpA, and it is to these zones that the listed values refer. The second test is an adaption of Student's *t*-test, according to which the probability that many of the tabulated symmetries might have occurred as a random event was <10⁻⁶.

^b Number of particles approved by the OMO algorithm (Unser *et al.*, 1986) and used for averaging.

^c Resolution was determined using the spectral-signal-to-noise criterion (Unser *et al.*, 1987).

^d Numbers refer to four independent data sets of ClpP particles analyzed, and two each of ClpP(SA), ClpA *en face*, ClpA side view, and the 2:1 ClpAP complex. The full data set ClpP-1 consisted of 216 particles of which 177 were approved by OMO and whose average is shown in Figure 1d. The quoted parameters are for a subset of 98 images selected on the grounds that their individual rotational power spectra each showed dominant 7-fold harmonics. This averaged image (not shown) was very similar to that in Figure 1d except that the 7-fold symmetry around the periphery was conveyed with somewhat greater contrast. The full data set, unbiased by such selection, probably includes some non-*en face* views which are difficult to recognize as such because ClpP is, to a first approximation, a hollow sphere whose projections all resemble each other (see the text).

^e The 2:1 ClpAP complex has two hexamers of ClpA flanking a central tetradecamer of ClpP.

^f The 1:1 ClpAP complex has a single hexamer of ClpA axially aligned with tetradecameric ClpP.

^g NA, not applicable.

on one side. We take the latter images to be side views. Image analysis of the *en face* views revealed a statistically significant 6-fold symmetry (Table 1), and no evidence of 7-fold symmetry. An averaged *en face* image is shown in Figure 1h. The 6-fold symmetry was strong enough to be detected only around the periphery, and the peripheral parts of the averaged images of ClpA were quite reproducible, whereas the inner parts were only faintly contrasted and somewhat variable. We expect that the appearance of this part of the *en face* projection should depend to some extent on how well the fuzzy

terminal mass seen in side view is preserved and stained.

ClpA is similar to the highly homologous yeast Clp-type chaperonin, Hsp104 (Parsell *et al.*, 1994), in forming a particle with 6-fold symmetry, but the stain-accumulating central region seen with the latter molecule is much less evident for ClpA. Taking into account its molecular weight and rotational symmetry, ClpA must be a hexamer. Figure 1i shows the averaged side view of ClpA, which is evidently polar, with two parallel striations of high density and a smaller, amorphous mass adjacent to one of the

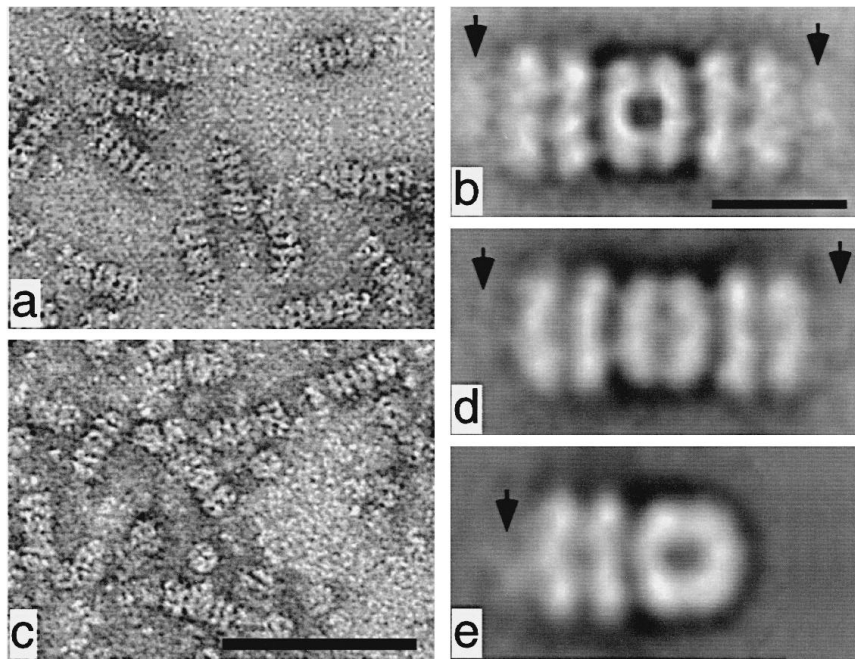


Figure 2. Electron micrographs of ClpAP complexes. Specimen preparation, microscopy, and image averaging were performed as described in the legend to Figure 1. a, A typical field of the ClpAP complexes formed with ClpA in excess of ClpP. ClpAP was prepared by mixing 100 $\mu\text{g/ml}$ ClpA and 20 $\mu\text{g/ml}$ ClpP in the presence of 2 mM $\text{ATP}\gamma\text{S}$ and 20 mM MgCl_2 in the buffer described in Figure 1. A molar excess of ClpA hexamers over ClpP tetramers favors a complex in which two ClpA hexamers are bound to one ClpP tetradecamer. Bar represents 50 nm. b, Computer averaged image of the 2:1 ClpAP complex obtained by averaging 68 molecules after rotational and translational alignment. Complexes that were slightly curved were computationally straightened (Kocsis *et al.*, 1991) before image averaging. The complexes are seen almost exclusively in side view and show a central double striation contributed by ClpP flanked on either side by the structural motif of double striations plus a smaller additional mass that corresponds to a side view of ClpA. c, A typical field of 2:1 complexes of ClpA and ClpP(SA). ClpP(SA) was complexed with ClpA as described above. In this experiment, the terminal masses were not so well contrasted, presumably as a consequence of the particular staining conditions pertaining in this experiment, and possibly also of radiation damage. Nevertheless, this feature has been reproducibly visualized in a great many non-averaged micrographs, as well as in averaged images (Figure 1i; a second independent average, not shown; and Figure 2b and e), and we conclude that it represents a genuine component of ClpA. d, Computer averaged image of 57 complexes of ClpA with ClpP(SA). The central two striations contributed by the ClpP(SA) molecules are evident, as is the additional stain-excluding mass between the rings contributed by the propeptide. Bar represents 10 nm. e, Computer averaged image of the 1:1 ClpAP complex. ClpA and ClpP were mixed as described above but ClpA and ClpP were each present at 50 $\mu\text{g/ml}$. Under these conditions, a 1:1 complex of ClpA hexamers to ClpP tetradecamers is favored.

striations. These data imply that the ClpA monomer consists of two major domains of approximately equal size, together with a third, smaller domain. Thus, each striation represents the side-projection of a ring of six copies of one of the major domains, and the striations are resolved by the penetration of stain into a circumferential groove around this ring of six bilobed subunits. The terminal mass is assigned to the smaller third domains. The inferred organization of ClpA into domains is consistent with sequence analysis that indicates that ClpA and other Clp family members in prokaryotes and eukaryotes arose by fusion of two large, evolutionarily distinct domains both of which bind ATP (Gottesman *et al.*, 1990).

Complexes of ClpAP were obtained by mixing the two proteins in the presence of $\text{ATP}\gamma\text{S}$ and Mg (Maurizi, 1991; Singh & Maurizi, 1994). Electron micrographs of complexes formed with an excess of ClpA over ClpP show particles with six parallel striations and a small amorphous mass at either end

(Figure 2a). Presumably, they represent side views. After averaging (Figure 2b), the complex is seen to have two mirror-symmetric central striations flanked on both sides by slightly longer double striations with an amorphous mass on the distal side. The latter features are indistinguishable from side views of ClpA alone (cf. Figure 1h). The length of the two middle striations, ~ 11 nm, matches the diameter of ClpP, and we infer that they represent a side view of ClpP for the following reasons. First, the two striations appear to be mirror-symmetric, which would not be the case if a partially split heptameric ring were viewed *en face*. Second, complexes of ClpA with ClpP(SA) show only parallel striations (cf. Figure 2c and d), without the dense central staining seen when the ClpP(SA) is viewed *en face* (Figure 1e). Third, if ClpA and ClpP rings were bound orthogonally, complexes oriented to present a side view of ClpP would produce projections with one or more ClpP striations perpendicular to the ClpA striations; however, such views are never seen.

Fourth, given the 7-fold symmetry of ClpP, an interpretation of the observed projection of the ClpP molecule in complex as *en face* is not easily reconciled with the exclusive attachment of ClpA molecules to ClpP at two positions 180 degrees apart.

The morphology of ClpP in the complex helps explain why side views, readily observed for ClpA, were not easily recognized in ClpP preparations. ClpP, with an average diameter of ~11 nm and a height of ~10 nm, is an approximately spherical molecule, with a hollow, stain-penetrable core. Such a molecule presents an annular appearance when viewed in projection from any angle, including the *en face* and side views. Nevertheless, the consistency with which 7-fold symmetry was observed in unbiased sampling of populations of ClpP molecules indicates that ClpP tends to adsorb to carbon films in the *en face* projection.

The arrangement of subunits of ClpP is similar to that of the inner (beta-type) subunits of the eukaryotic and archaeal proteasomes (Zwickl *et al.*, 1990) and is reminiscent of the bipolar 7-fold-symmetric structures of GroEL and other Hsc60 chaperonins (Hohn *et al.*, 1979; Langer *et al.*, 1992). In the complex the ClpP and ClpA rings are aligned axially to form a barrel-like structure strikingly similar to that observed for the 20 S proteasome complexed with either the 19 S ATP-binding particles (Peters *et al.*, 1993; Schauer *et al.*, 1993) or the non-ATP-binding P28 activator (Gray *et al.*, 1994). The side view of ClpA in the ClpAP complex is asymmetric and similar to that of ClpA alone. The heptameric rings of ClpP should thus be isologously bonded to each other, and their distal surfaces interact with ClpA through the domains of ClpA that form the ring distal to the amorphous mass. We infer that the interacting domains may represent the carboxy termini of ClpA (Figure 3).

The heavy staining in the central region of ClpP in side-projection as seen in the complex (Figure 2b) is striking. This feature is also seen in *en face* projections of ClpP (Figure 1d). It is, however, generally absent from the corresponding regions of ClpP(SA), as seen complexed with ClpA (Figure 2c and d), or in isolation in the *en face* view (Figure 1e). It seems reasonable to attribute the additional stain-excluding mass in ClpP(SA) to the propeptide, i.e. the stained region visible in both the *en face* and side views of ClpP represents a solvent-accessible internal cavity that is either filled or occluded by the propeptide in ClpP(SA). Because propeptides are often competitive inhibitors of their respective proteases and may occupy a groove adjacent to the proteolytic active site in protease zymogens (Baker *et al.*, 1992), these data also suggest that the active sites of ClpP may be disposed about the central axis in relatively close proximity to each other.

When ClpP is present in excess over ClpA, a complex of one tetradecamer of ClpP with one hexamer of ClpA is seen (Figure 2e). This 1:1 complex appears as a discrete species in gel filtration and sedimentation analyses (Maurizi, 1991; Maurizi & Ginsburg, 1995), and assays of ATP-dependent

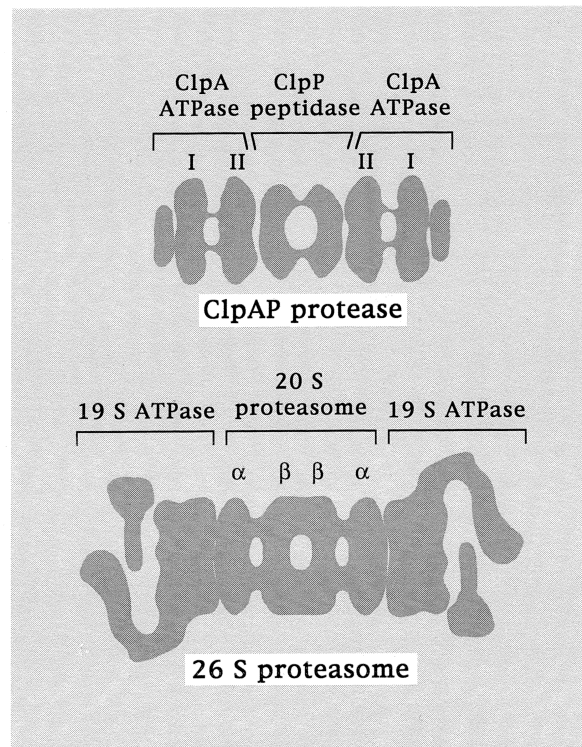


Figure 3. Schematic representations of the 2:1 ClpAP protease complex and the 26 S proteasome showing the close similarity in overall architecture and location of the respective oligomers. ClpA and ClpP in the complex were identified by reference to their appearance in micrographs of the individual proteins (see the text). Domain I (amino-terminal) and domain II (carboxy-terminal) of ClpA are tentatively assigned based on the expected larger size of domain I (Gottesman *et al.*, 1990) and indirect evidence that domain II interacts with ClpP (Singh & Maurizi, 1994). The proteasome rendition is based on negatively stained electron micrographs as described by Peters *et al.* (1993). The alpha and beta rings were assigned by analogy to the archaeal proteasome (Zwickl *et al.*, 1990; Schauer *et al.*, 1993).

degradation in the presence of excess ClpP indicate that the 1:1 complex is enzymatically active (Maurizi *et al.*, 1994). The ClpP ring not in contact with ClpA has a markedly more concave or bowed appearance than the other ring. This difference suggests that ClpP may undergo a conformational change upon interaction with ClpA. However, we cannot yet rule out the possibility that this effect may arise, at least in part, from the two ClpP rings not being in equivalent staining environments (i.e. the stain is generally shallower around the ring that is not in contact with ClpA, and the ring that is in contact with ClpA may be supported against drying-induced flattening by that interaction). In the context of the putative conformational change in ClpP, we note that an induced asymmetry has also been observed in the chaperonin, GroEL upon binding of the cofactor GroES at one end (Chen *et al.*, 1994), but no such effect was reported for single-end binding of the 19 S complex to the 20 S proteasome (Peters *et al.*, 1993).

In comparing the structure of the ClpAP protease with the 26 S eukaryotic proteasome (Peters *et al.*, 1993) and the 20 S archaeal proteasome (Zwickl *et al.*, 1990), some striking similarities are evident (Figure 3). The 20 S proteasome or multicatalytic proteinase, which is ubiquitous in eukaryotic cells, forms the proteolytic core of the 26 S proteasome ($M_r \approx 2 \times 10^6$) responsible for the ATP-dependent degradation of ubiquitinated proteins (Peters *et al.*, 1993). The ClpAP complex and the proteasome are similar in overall dimensions. Both complexes have as their central element a bipolar, double-ring, 7-fold-symmetric protease. In both ClpAP and the 26 S proteasome, an oligomeric ATPase is attached to one or both opposed rings of the protease. There is virtually no sequence homology between ClpP and the proteolytic subunits of the proteasome and only a limited similarity between the ATPase binding site of ClpA and the ATPase components of the 26 S proteasome (Dubiel *et al.*, 1992). The eukaryotic protease has a larger number of functionally distinct components, e.g. isopeptidase activity and several classes of proteolytic active sites. Nevertheless, the overall structural resemblance between ClpAP and the 26 S proteasome suggests that there are similarities in the underlying biochemical mechanisms by which these enzymes bind, unfold, and deliver protein substrates to their proteolytic active sites.

A double ring with 7-fold symmetry is the basic organizational principle, not only of the 20 S proteasome (Zwickl *et al.*, 1990), essential for cytosolic protein degradation, but also of the GroEL bacterial chaperonin (Hohn *et al.*, 1979), which is involved in protein remodeling in the cell. The finding that eubacterial ClpP, the proteolytic component of a major cytoplasmic ATP-dependent protease, also forms a double ring with 7-fold symmetry suggests that this arrangement of subunits may define a group of evolutionarily distinct but structurally related proteins that function in protein remodeling and/or degradation. These examples suggest that a 7-fold-symmetric structure may provide some advantage in catalytic efficiency or processivity for enzymes that make repeated contacts with similar but non-identical substrates or regions of macromolecular substrates.

In active complexes, 6-fold-symmetric ClpA interacts with 7-fold-symmetric ClpP, resulting in a symmetry mismatch in their axial stacking. This mismatch rules out simple models of one-to-one correspondence in activities of ClpA and ClpP subunits, and is consistent with data indicating that all ClpP subunits are not active simultaneously (Thompson *et al.*, 1994). In the complex, ClpP and ClpA subunits are in non-equivalent conformations, which might produce slight alterations in substrate recognition and binding at the active sites. A comparable symmetry mismatch has been observed at the bacteriophage head-tail junction (Hendrix, 1978) where the 6-fold-symmetric tail is joined to a 5-fold vertex of the capsid, via a 12- or 13-fold connector protein. More recently, the 3-fold symmet-

ric $\alpha_3\beta_3$ component of mitochondrial F1-ATP synthase was shown to make asymmetric contact with the γ subunit which forms a central spindle within the central cavity of the hexamer (Abrahams *et al.*, 1994). The observed asymmetry in ClpAP might have functional implications akin to the "binding change mechanism" proposed for F1-ATP synthase (Boyer, 1989), in which intrinsic asymmetry of interactions between the $\alpha_3\beta_3$ complex and non-stoichiometric γ subunit allows sequential catalysis at the three active sites as the γ chain rotates within the central channel (Abrahams *et al.*, 1994). Enzymatic data show that ClpAP does not dissociate in the time of turnover of several molecules of protein substrate (S. K. Singh & M. R. Maurizi, unpublished results), but changes in bonding contact between ClpA and ClpP in response to ATP hydrolysis could cause ClpA and ClpP to rotate about their common axis. We conjecture that, as protein substrates are bound and partly released from ClpA during cycles of ATP hydrolysis, rotation of ClpA and ClpP results in a "ratcheting" or "corkscrewing" effect that facilitates movement of protein substrates into the active sites of ClpP.

Acknowledgements

The authors thank Dr Blair Bowers (NHLBI, NIH) for providing us with electron micrographs of ClpP for comparison to those obtained in this study. The assistance of Dr Mark Thompson in purifying ClpA and ClpP is greatly appreciated. The authors thank Drs Ann Ginsburg, Craig Hyde and Vaidehi Sridhar for helpful discussions, and Drs J. Flanagan and J. Wall (Brookhaven National Laboratory) for communicating their results on the oligomeric structure of ClpP prior to publication.

References

- Abrahams, J. P., Leslie, A. G. W., Lutter, R. & Walker, J. E. (1994). Structure at 2.8 Å resolution of F1-ATPase from bovine heart mitochondria. *Nature*, **370**, 621–628.
- Baker, D., Silen, J. L. & Agard, D. A. (1992). Protease pro region required for folding is a potent inhibitor of the mature enzyme. *Proteins: Struct. Funct. Genet.* **12**, 339–344.
- Boyer, P. D. (1989). A perspective on the binding change mechanism for ATP synthesis. *FASEB J.* **3**, 2164–2178.
- Carrascosa, J. L. & Steven, A. C. (1978). A procedure for evaluation of significant structural differences between related arrays of protein molecules. *Micron*, **9**, 199–206.
- Chen, S., Roseman, A. M., Hunter, A. S., Wood, S. P., Burston, S. G., Ranson, N. A., Clarke, A. R. & Saibil, H. R. (1994). Location of a folding protein and shape changes in GroEL-GroES complexes imaged by cryo-electron microscopy. *Nature*, **371**, 261–264.
- Dubiel, W., Ferrell, K., Pratt, G. & Rechsteiner, M. (1992). Subunit 4 of the 26 S protease is a member of a novel eukaryotic ATPase family. *J. Biol. Chem.* **267**, 22699–22702.
- Gottesman, S. & Maurizi, M. R. (1992). Regulation by proteolysis: energy-dependent proteases and their targets. *Microbiol. Rev.* **56**, 592–621.

- Gottesman, S., Squires, C., Pichersky, E., Carrington, M., Hobbs, M., Mattick, J. S., Dalrymple, B., Kuramitsu, H., Shiroza, T., Foster, T., Clark, W. P., Ross, B., Squires, C. L. & Maurizi, M. R. (1990). Conservation of the regulatory subunit for the Clp ATP-dependent protease in prokaryotes and eukaryotes. *Proc. Natl Acad. Sci. USA*, **87**, 3513–3517.
- Gray, C. W., Slaughter, C. A. & DeMartino, G. N. (1994). PA28 activator protein forms regulatory caps on proteasome stacked rings. *J. Mol. Biol.* **236**, 7–15.
- Hendrix, R. W. (1978). Symmetry mismatch and DNA packaging in large bacteriophages. *Proc. Natl Acad. Sci. USA*, **75**, 4779–4783.
- Hershkov, A. & Ciechanover, A. (1992). The ubiquitin system for protein degradation. *Annu. Rev. Biochem.* **61**, 761–807.
- Hohn, T., Hohn, B., Engel, A., Wurtz, M. & Smith, P. R. (1979). Isolation and characterization of the host protein GroE involved in bacteriophage lambda assembly. *J. Mol. Biol.* **129**, 359–373.
- Kocsis, E., Trus, B. L., Steer, C. J., Bisher, M. E. & Steven, A. C. (1991). Image averaging of fibrous, flexible macromolecules: the clathrin triskelion has an elastic proximal segment. *J. Struct. Biol.* **107**, 6–14.
- Kocsis, E., Trus, B. L., Cerritelli, M., Cheng, N. & Steven, A. C. (1995). Improved methods for determination of rotational symmetries in macromolecules. *Ultramicroscopy*, in the press.
- Langer, T., Pfeifer, G., Martin, J., Baumeister, W. & Hartl, F.-U. (1992). Chaperonin-mediated protein folding: GroES binds to one end of the GroEL cylinder which accommodates the protein substrate within its central cavity. *EMBO J.* **11**, 4757–4765.
- Maurizi, M. R. (1991). ATP-promoted interaction between ClpA and ClpP in activation of Clp protease from *Escherichia coli*. *Biochem. Soc. Trans.* **19**, 719–723.
- Maurizi, M. R. (1992). Proteases and protein degradation in *Escherichia coli*. *Experientia*, **48**, 178–201.
- Maurizi, M. R. & Ginsburg, A. (1995). Hydrodynamic properties of the ATP-dependent ClpAP protease of *E. coli*. *Biophys. J.* **68**, A404.
- Maurizi, M. R., Clark, W. P., Katayama, Y., Rudikoff, S., Pumphrey, J., Bowers, B. & Gottesman, S. (1990a). Sequence and structure of ClpP, the proteolytic component of the ATP-dependent Clp protease of *Escherichia coli*. *J. Biol. Chem.* **265**, 12536–12445.
- Maurizi, M. R., Clark, W. P., Kim, S.-H. & Gottesman, S. (1990b). ClpP represents a unique family of serine proteases. *J. Biol. Chem.* **265**, 12546–12552.
- Maurizi, M. R., Thompson, M. W., Singh, S. K. & Kim, S.-H. (1994). Endopeptidase Clp: the ATP-dependent Clp protease from *Escherichia coli*. *Methods Enzymol.* **244**, 314–331.
- Parsell, D. A., Kowal, A. S. & Lindquist, S. (1994). *Saccharomyces cerevisiae* Hsp104 protein. Purification and characterization of ATP-induced structural changes. *J. Biol. Chem.* **269**, 4480–4487.
- Peters, J.-M., Cejka, Z., Harris, J. R., Kleinschmidt, J. A. & Baumeister, W. (1993). Structural features of the 26 S proteasome complex. *J. Mol. Biol.* **234**, 932–937.
- Schauer, T. M., Nesper, M., Kehl, M., Lottspeich, F., Muller-Taubenberger, A., Gerisch, G. & Baumeister, W. (1993). Proteasomes from *Dictyostelium discoideum*: characterization of structure and function. *J. Struct. Biol.* **11**, 135–147.
- Singh, S. K. & Maurizi, M. R. (1994). Mutational analysis demonstrates different functional roles for the two ATP-binding sites in ClpAP protease from *Escherichia coli*. *J. Biol. Chem.* **269**, 29537–29545.
- Thompson, M. W., Singh, S. K. & Maurizi, M. R. (1994). Processive degradation of proteins by the ATP-dependent Clp protease from *Escherichia coli*: requirement for the multiple array of active sites in ClpP but not ATP hydrolysis. *J. Biol. Chem.* **169**, 18209–18215.
- Trus, B. L., Unser, M., Pun, T. & Steven, A. C. (1992). Digital image processing of electron micrographs: the PIC system II. *Scanning Microsc. Suppl.* **6**, 441–451.
- Unser, M., Trus, B. L. & Steven, A. C. (1986). Odd men out: a quantitative objective procedure for identifying anomalous members of a set of noisy images of ostensibly identical specimens. *Ultramicroscopy*, **19**, 337–347.
- Unser, M., Trus, B. L. & Steven, A. C. (1987). A new resolution criterion based on spectral signal-to-noise ratios. *Ultramicroscopy*, **23**, 39–51.
- Wickner, S., Gottesman, S., Skowrya, D., Hoskins, J., McKenney, K. & Maurizi, M. R. (1994). A new molecular chaperone, ClpA, functions like DnaK and DnaJ. *Proc. Natl Acad. Sci. USA*, **91**, 12218–12222.
- Zwickl, P., Pfeifer, G., Lottspeich, F., Kopp, F., Dahlmann, B. & Baumeister, W. (1990). Electron microscopy and image analysis reveal common principles of organization in two large protein complexes: groEL-type proteins and proteasomes. *J. Struct. Biol.* **103**, 197–203.

Edited by A. Klug

(Received 30 December 1994; accepted in revised form 23 May 1995)